Experimental Neurology 216 (2009) 383–389

Contents lists available at ScienceDirect

Experimental Neurology

journal homepage: www.elsevier.com/locate/yexnr

Mexiletine-responsive erythromelalgia due to a new $Na_v1.7$ mutation showing use-dependent current fall-off

Jin-Sung Choi [a,b,c], Lili Zhang [d], Sulayman D. Dib-Hajj [a,b,c], Chongyang Han [a,b,c,e], Lynda Tyrrell [a,b,c], Zhimiao Lin [d], Xiaoliang Wang [e], Yong Yang [a,b,c,d,*], Stephen G. Waxman [a,b,c,*]

[a] Department of Neurology, Yale University School of Medicine, New Haven, CT 06510, USA
[b] Center for Neuroscience and Regeneration Research, Yale University School of Medicine, New Haven, CT 06510, USA
[c] Rehabilitation Research Center, VA Connecticut Healthcare System, West Haven, CT 06516, USA
[d] Department of Dermatology, Peking University First Hospital, Beijing 100034, China
[e] Institute of Materia Medica, Chinese Academy of Medical Sciences and Peking Union Medical College, Beijing 100050, China

ARTICLE INFO

Article history:
Received 17 September 2008
Revised 15 December 2008
Accepted 17 December 2008
Available online 31 December 2008

Keywords:
Inherited neuropathy
Channelopathy
Pain
Erythermalgia
Sodium channel blockers
Local anesthetics

ABSTRACT

Inherited erythromelalgia (IEM), characterized by episodic burning pain and erythema of the extremities, is produced by gain-of-function mutations in sodium channel $Na_v1.7$, which is preferentially expressed in nociceptive and sympathetic neurons. Most patients do not respond to pharmacotherapy, although occasional reports document patients as showing partial relief with lidocaine or mexiletine. A 7-year-old girl, with a two-year history of symmetric burning pain and erythema in her hands and feet, was diagnosed with erythromelalgia. Treatment with mexiletine reduced the number and severity of pain episodes. We report here a new IEM $Na_v1.7$ mutation in this patient, and its response to mexiletine. SCN9A exons from the proband were amplified and sequenced. We identified a single nucleotide substitution (T2616G) in exon 15, not present in 200 ethnically-matched control alleles, which substitutes valine 872 by glycine (V872G) within DII/S5. Whole-cell patch-clamp analysis of wild-type and mutant $Na_v1.7$ channels in mammalian cells show that V872G shifts activation by −10 mV, slows deactivation, and generates larger ramp currents. We observed a stronger use-dependent fall-off in current following exposure to mexiletine for V872G compared to wild-type channels. These observations suggest that some patients with IEM may show a favorable response to mexiletine due to a use-dependent effect on mutant $Na_v1.7$ channels. Continued relief from pain, even after mexiletine was discontinued in this patient, might suggest that early treatment may slow the progression of the disease.

Introduction

Sodium channel $Na_v1.7$ has emerged as a major contributor to pain based upon recent genetic and electrophysiological studies that have identified a link between this channel isoform and nociceptive DRG neuron hyperexcitability (Dib-Hajj et al., 2007; Waxman, 2007). Autosomal dominant gain-of-function mutations in $Na_v1.7$ that shift activation in a hyperpolarizing direction produce inherited erythromelalgia (IEM) (Cummins et al., 2004; Dib-Hajj et al., 2005; Choi et al., 2006; Han et al., 2006; Harty et al., 2006; Lampert et al., 2006; Rush et al., 2006; Sheets et al., 2007; Cheng et al., 2008), and autosomal dominant $Na_v1.7$ mutants that impair inactivation cause paroxysmal extreme pain disorder (PEPD) (Fertleman et al., 2006). Three IEM mutations (Dib-Hajj et al., 2005; Harty et al., 2006; Rush et al., 2006) and two PEPD mutations (Dib-Hajj et al 2008; Estacion et al., 2008) have been studied by current clamp and have been shown to cause hyperexcitability of DRG neurons. In contrast, autosomal recessive loss-of-function mutations of $Na_v1.7$ lead to congenital indifference to pain (Cox et al., 2006; Ahmad et al., 2007; Goldberg et al., 2007). Because of these links to human pain disorders, $Na_v1.7$ has become an attractive target for the development of new and more effective pain therapeutics.

Symptoms of IEM usually persist throughout life after the disease becomes clinically manifest, and are characterized by episodes of burning pain triggered by mild warmth or exercise, together with erythema and mild swelling in the hands and feet (Dib-Hajj et al., 2007; Drenth and Waxman, 2007). Cooling of the affected extremities produces relief of the symptoms of erythromelalgia. While pharmacological therapies (including treatment with sodium channel blockers) is usually ineffective, treatment with local anesthetics has been reported to be partially effective in a small number of

* Corresponding authors. S.G. Waxman is to be contacted at Department of Neurology, LCI 707, Yale School of Medicine, New Haven, CT 06510, USA. Fax: +1 203 785 7826. Y. Yang, Department of Dermatology, Peking University First Hospital, Xicheng District, Beijing 100034, China.
E-mail addresses: dryongyang@bjmu.edu.cn (Y. Yang), stephen.waxman@yale.edu (S.G. Waxman).

0014-4886/$ – see front matter © 2008 Elsevier Inc. All rights reserved.
doi:10.1016/j.expneurol.2008.12.012

patients with erythromelalgia, including IEM (Nathan et al., 2005; Harty et al., 2006).

We report here the identification of a new mutation in a sporadic case of IEM, in a patient who showed sustained improvement during and after a one month period of treatment with the lidocaine derivative mexiletine. Exon screening identified a substitution of valine with glycine at position 872 (V872G), a highly conserved residue within the distal end of segment 5 in domain II (DII/S5) of the channel. Whole-cell patch clamp analysis shows that $Na_v1.7$/V872G shifts the activation voltage-dependence by −10 mV, slows deactivation, and generates enhanced ramp currents. Notably, we observed a stronger use-dependent fall-off of current for V872G channels following exposure to mexiletine compared to wild-type channels. The increased sensitivity of V872G to use-dependent effects of mexiletine appears to underlie this patient's favorable response to this sodium channel blocker.

Methods

Patient

The patient is an adopted 7-year-old girl. Family consent was obtained according to the institutional review board protocol and blood samples were then withdrawn and analyzed for mutations in *SCN9A*.

Exon screening

Genomic DNA was extracted from blood samples of the patient. PCR amplification of the 26 exons of *SCN9A* was performed and the amplicons were purified and sequenced as previously described (Yang et al., 2004). Genomic sequences were compared to reference $Na_v1.7$ cDNA (Klugbauer et al., 1995) to identify sequence variation.

Plasmids and transfection

The plasmid carrying the wild-type human $Na_v1.7_R$ insert and methods to introduce the mutation have been described previously (Cummins et al., 2004; Dib-Hajj et al., 2005; Han et al., 2006). Wild-type $hNa_v1.7_R$ or V872G mutant channels were cotransfected with the human β1 and β2 subunits (Lossin et al., 2002) into human embryonic kidney (HEK293) cells using Lipofectamine 2000 according to manufacturer recommendations, and currents were recorded 24 h later.

Whole-cell patch-clamp recordings

Whole-cell patch-clamp recordings were performed at room temperature with Axopatch 200B amplifiers (Molecular Devices, Foster City, CA) using the following solution: internal (mM), 140 CsF, 1 EGTA, 10 NaCl, and 10 HEPES, pH 7.3, adjusted to 310 mOsmol/l with sucrose and CsOH; external (mM), 140 NaCl, 3 KCl, 1 $MgCl_2$, 1 $CaCl_2$, 10 glucose, 20 HEPES, pH 7.3, adjusted to 320 mOsmol/l with sucrose and NaOH. Recordings were started 4 min after establishing whole-cell configuration to allow currents to stabilize. Currents were elicited from a holding potential of −120 mV, filtered at 5 kHz, and acquired at 50 kHz using pClamp 8.2 (Axon Instruments). Voltage errors were minimized using 90% series resistance compensation in all recordings. The liquid junction potential was not corrected.

Drug application

Mexiletine hydrochloride (Sigma, St Louis, MO) was dissolved in standard external recording solution (see above) to give a stock solution of 10 mM. Subsequent dilutions were performed in standard bathing solution to give concentrations of (mM); 0.1, 0.3, 1, and 3. Mexiletine solutions were made fresh before patch-clamp recordings and applied through a gravity-driven system with perfusion pencil (Automate Scientific, Berkeley, CA) allowing a rapid perfusion of the recording chamber. During the recording, the cells were continuously perfused with test solution. Concentration–response data were best fitted with the following logistic equation using Origin 7.5 software (Microcal Software Inc., Northampton, MA). $Y = 1 / [1 + IC_{50} / M]^n$ where IC_{50} is the concentration of mexiletine resulting in 50% inhibition, M is the concentration of mexiletine and n is the Hill coefficient.

Student's unpaired t tests were used with the criterion for statistical significance set at 0.05. Descriptive data are presented as the mean±SEM. Data were analyzed using Clampfit 8.2 software and Origin 7.5.

Results

Clinical description

A 7-year-old girl from China presented to the clinic with complaints of burning pain and flare with light itching in feet and hands. Age of onset of the symptoms was 5-year-old and the symptoms were severe at the onset. The patient was an adopted child, so family history of biological parents was not available. The patient reported daily pain episodes, triggered by warmth, which could be relieved by soaking the feet in ice-cold water, and she could not wear shoes or tolerate a blanket at night. Blood tests, including a complete blood count, basic metabolic panel, liver function tests, antinuclear antibodies, and C-reactive protein yielded normal results. Pharmacotherapy using paracetamol or aspirin, and traditional Chinese herbs were tried without success. The patient was diagnosed with erythromelalgia. The symptoms responded favorably to mexiletine 300 mg/day. Although less severe symptoms could be exacerbated by heat or occasional exercise, the frequency, duration, and intensity of the patient's pain episodes decreased upon treatment. However, the patient's parents suspended treatment after one month because of fear of potential side effects. The parents reported continued improvement of the symptoms even 1 year after suspension of treatment, with the patient able to tolerate pain, wear shoes and use blankets at night.

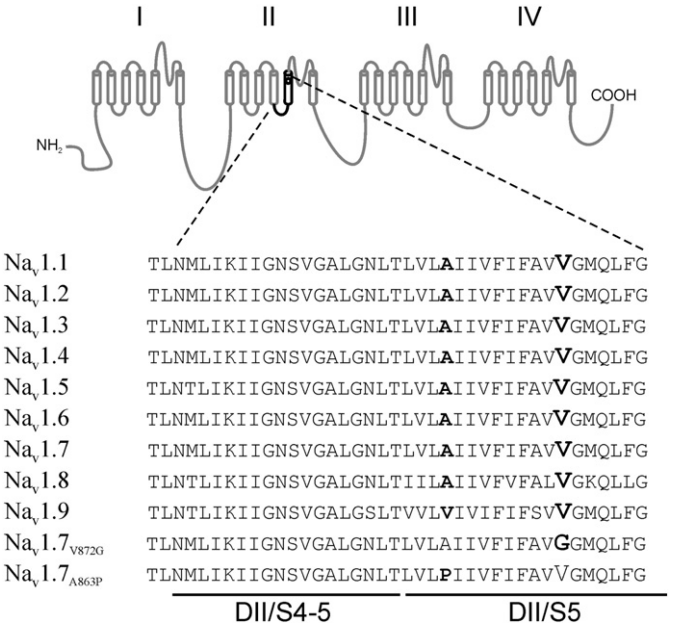

Fig. 1. Schematic of a voltage-gated sodium channel showing the location of the V872G mutation and the aligned sequences for the Na_v1 DII/S4-S5 linker and DII/S5. V872 is conserved in the nine members of the Na_v1 family of voltage-gated sodium channels. A863P, the other erythromelalgia mutation in DII/S5, is shown in bold for comparison.

Mutation in exon 15

Sequence analysis of *SCN9A* demonstrated a T to G substitution (c. 2616T>G) in exon 15 in the proband. This single nucleotide mutation causes the substitution of valine 872 with glycine (V872G) in transmembrane segment 5 in domain II (Fig. 1). This substitution was not found in 200 alleles from normal Chinese controls, indicating that this mutation is not a polymorphism.

V872G mutation lowers voltage for activation but not inactivation

Wild-type (WT) $hNa_v1.7_R$ and the mutant channel $hNa_v1.7_R$/V872G (V872G) were transiently expressed together with hβ1 and hβ2 subunits in HEK293 cells. Figs. 2A and B show representative sodium currents recorded from cells expressing WT and V872G channels, respectively. Peak current densities of WT (379±76 pA/pF; n=16) and V872G (342±74 pA/pF; n=20) were not significantly different. The voltage-dependence of activation was examined using a series of depolarizing test pulses from −80 mV to +40 mV from a holding potential of −120 mV. As seen in the mean normalized current–voltage relationships (Fig. 2C), WT channels activate at potentials positive to −50 mV and peak near −5 mV, while V872G channels activate at potentials positive to −65 mV and peak near −15 mV. The peak and threshold of activation voltages of V872G current were hyperpolarized by ~10 mV, compared to WT currents. The reversal potentials for WT and V872G current were 70.2±0.8 mV (n=11) and 68.3±0.6 mV (n=15), indicating no change of ion selectivity. When the voltage-dependent activation curves were fitted with Boltzmann function (Fig. 2D), the midpoint of activation of V872G (−30.1±1.8 mV; n=12) was found to be significantly more hyperpolarized than in WT (−20.8±1.7 mV; n=9) without a change of the slope (WT, 7.6±0.4 mV; V872G, 7.6±0.2 mV).

In contrast to the differences in the voltage-dependence of activation, the voltage dependence of steady-state inactivation was similar for WT and V872G channels (Fig. 2D). The midpoint of steady-state inactivation (measured with 500 ms prepulses) was not significantly different for WT (−80.8±2.1 mV; n=11) and V872G (−81.7±1.3 mV; n=13) channels. The slope of the steady-state inactivation curve for V872G (5.8±0.2 mV) was not significantly different from the slope for WT channels (6.1±0.2 mV) as well.

V872G mutation increases the rate of channel activation and of fast-inactivation at −20 to −30 mV, but not at voltages where the channels are fully activated

Because the change of voltage-dependence of activation may be accompanied by changes the kinetics of activation and inactivation, we compared the kinetics of activation, which reflect the transition from the closed to the open state, for WT and V872G channels by measuring time-to-peak (Fig. 3A). The rate of activation for V872G was faster than in WT channels at potentials ranging from −30 to 10 mV. The time constant of inactivation, which provides a measure of the open-to-inactivated transition, was estimated by monoexponential fit to the current from peak to end. The time constants for inactivation were faster for V872G than for WT channels between −30 and −20 mV (Fig. 3B), while the time constants of these channels were similar at more depolarized potentials where the channels are fully activated.

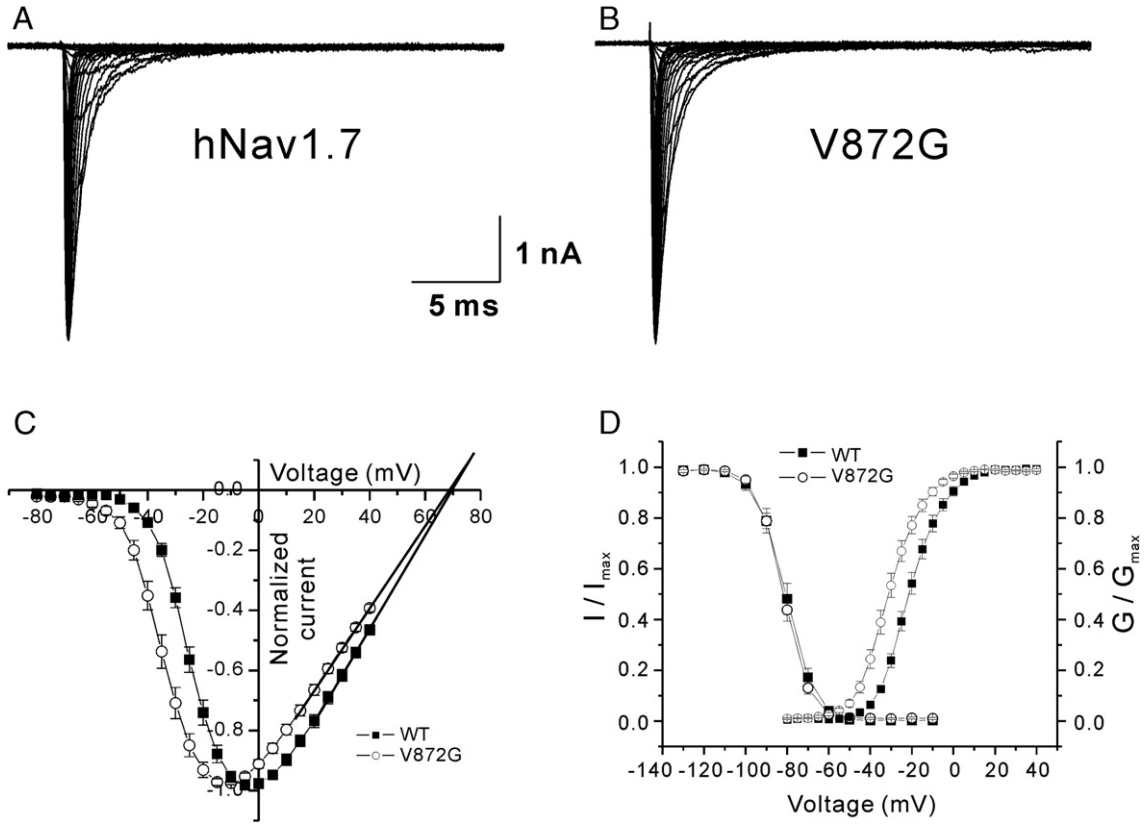

Fig. 2. Comparison of voltage-dependent activation for WT and V872G hNav1.7. Representative current traces recorded from HEK-293 cells that expressed WT (A) or V872G mutant (B) together with hβ1 and hβ2. Whole-cell Na^+ currents were elicited by 50-ms test pulses to potentials between −80 mV and +40 mV in steps of 5 mV from a holding potential of −120 mV. (C) Mean normalized I–V curves for WT (■, n=11) and V872G mutant (○, n=15). The reversal potential for each current was estimated by extrapolating the linear ascending segment of the I–V curve to the voltage axis. (D) Activation and steady-state inactivation curves in cells expressing for WT and V872G channels were fitted by Boltzmann distribution equations. The voltage-dependence of activation was examined using a series of depolarizing test pulses for 50 ms to +40 mV from a holding potential of −120 mV. For steady-state inactivation experiments, cells clamped at −120 mV were given 500-ms conditioning pulses to voltages between −130 mV and −10 mV followed by a test pulse to −10 mV. Normalized sodium currents (I/I_{max}) measured during test pulses were plotted against conditioning voltage.

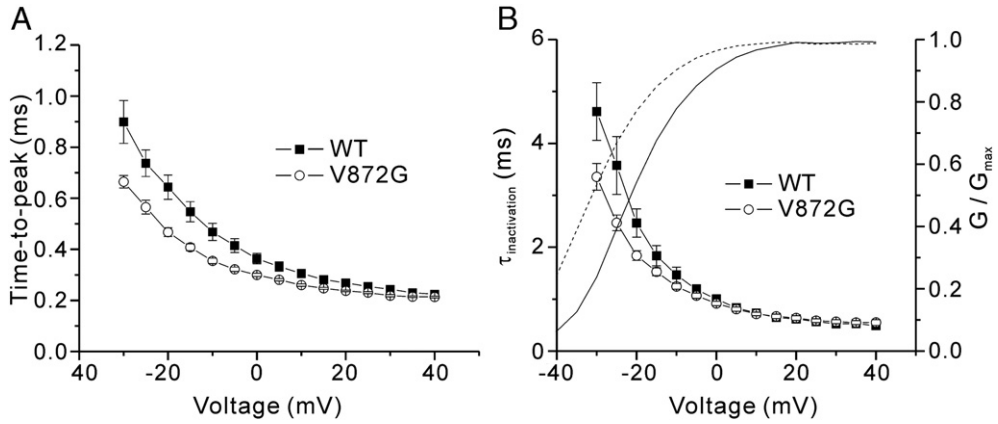

Fig. 3. (A) Time-to-peak as a function of test potentials for WT (■; $n=11$) and V872G mutant (○; $n=15$). (B) Fast inactivation kinetics as a function of voltage for WT ■; $n=11$) and V872G mutant (○; $n=15$). The currents were elicited as in Fig. 2 and fit with monoexponential function in the region from 90% of peak to zero current. Superimposed activation curves for WT (solid) and V872G mutant (dashed) (*Y*-axis on right) are the same as shown in Fig. 2D.

V872G mutation induces slower deactivation and an increase in ramp current

Kinetics of deactivation (Fig. 4A), which reflect the transition from the open to the closed state of WT and V872G channels, were also examined by eliciting tail currents at a range of potentials (from −120 to −40 mV) after briefly activating the channels (at −10 mV for 0.5 ms). V872G channels are characterized by a significantly longer time constant of deactivation (measured with monoexponential fits) at voltages more positive than −70 mV (Fig. 4A), indicative of slower deactivation of the mutant channels close to resting membrane potential of DRG neurons.

We examined the currents elicited in WT and V872G channels by slow ramp depolarizations (0.2 mV/ms from −100 to 0 mV over 500 ms). The ramp current for V872G channels was two-fold larger than for WT channels (Fig. 4B). Maximal amplitude of the peak current was 14.5±2.5 pA for WT channels ($n=11$), and 37.5±7.7 pA for V872G ($n=15$). Expressed as a percentage of peak current, the ramp currents were 0.29±0.09% for WT channels and 0.70±0.09% for V872G channels.

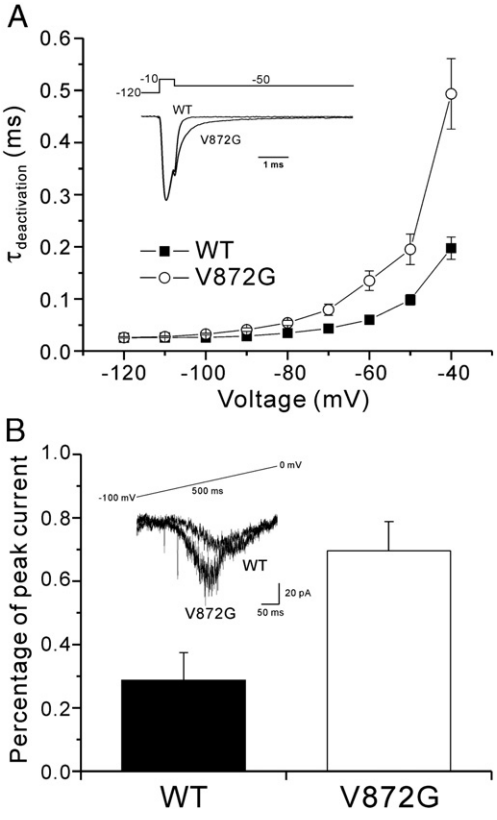

Fig. 4. Deactivation and ramp current properties for WT and V872G mutant. (A) Time constants for tail current deactivation at repolarization potentials ranging from −120 to −40 mV for WT (■; $n=7$) and V872G mutant (○; $n=9$). Cells were held at −120 mV and depolarized to −10 mV for 0.5 ms, followed by a repolarization to a range of potentials. Inset shows representative traces with repolarization to −50 mV for WT and V872G currents. (B) Comparison of ramp currents for WT and V872G mutant. Mean ramp current amplitude for V872G ($n=15$) is significantly larger than for WT ($n=11$) ($p<0.05$).

V872G mutation affects use-dependent effect of mexiletine

Finally, the block of WT and V872G channels by mexiletine was assayed by measuring the reduction of peak current elicited by depolarizing from −120 to −10 mV at a stimulation frequency of 0.2 Hz. Mexiletine reduced the peak amplitude of both WT and V872G currents in a concentration-dependent manner. The dose–response relationships for the blockade of mexiletine on WT and V872G channels are shown in Fig. 5A. Mexiletine produced a similar block of V872G peak current as compared to WT. The fits of concentration–response curves with a first-order binding function indicated that the half-maximal blocking concentration (IC_{50}) for V872G channels (0.46±0.03 mM) did not differ from that for WT channel (0.56±0.04 mM).

We also examined the use-dependent effect of mexiletine on the WT and V872G channels by depolarizing the transfected cells to −10 mV from a −120 mV holding potential at a frequency of 5 Hz in the absence and presence of mexiletine. Fig. 5B displays representative traces showing the use-dependent effect of WT (left) and V872G (right) currents in the absence or presence of 500 μM mexiletine, which is the IC_{50} for both WT and V872G currents. WT and V872G current amplitude were decreased to a similar degree (~12%) by the protocol in the absence of mexiletine (open symbols in Fig. 5C). However, the V872G current showed greater use-dependent fall-off compared to WT current beginning with the fifth pulse in the presence of 500 μM mexiletine, and maximal use-dependent current reduction at the 30th pulse in the presence of 500 μM mexiletine was stronger for V872G current (62.1±1.1%) than for WT current (51.4±2.3%, $p<0.01$).

Discussion

This study identifies a new mutation in *SCN9A*, the gene which encodes sodium channel $Na_v1.7$, in a patient with IEM who showed a favorable response to treatment with mexiletine. The new mutation

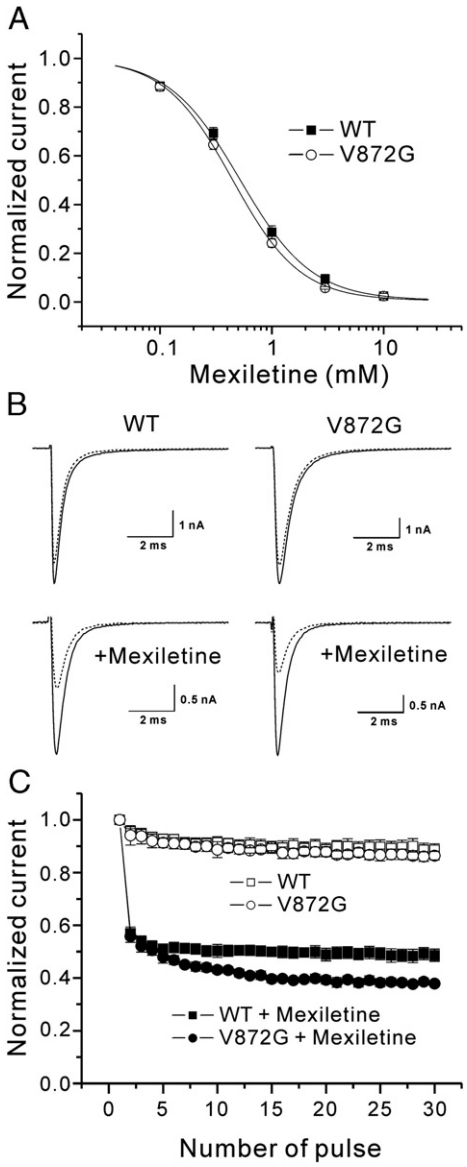

Fig. 5. Concentration and use-dependent effect of mexiletine on WT and V872G currents. (A) Whole-cell currents were elicited by 50 ms voltage steps to −10 mV from a holding potential of −120 mV at 5 sec intervals. The IC_{50} value for WT was 0.56± 0.04 mM and a Hill coefficient was 1.42 (n=6). The IC_{50} value for V872G was 0.46± 0.03 mM and a Hill coefficient was 1.43 (n=6). (B) Examples of peak WT (left) and V872G (right) currents from the first pulse (solid) to the last pulse (30th, dashed) during high frequency stimulation, depolarizing the transfected cells to −10 mV for 50 ms from −120 mV of holding potential at a frequency of 5 Hz, under control conditions (upper) and in the presence of 500 μM mexiletine (lower). (C) Use-dependent fall-off of peak WT (squares) and V872G (circles) currents in the absence (open symbols) or presence (closed symbols) of 500 μM mexiletine.

produces a single substitution of valine at codon 872 with glycine (V872G). V872 is conserved within the DII/S5 segment in the nine members of the voltage-gated sodium channel family, possibly reflecting a conserved functional role in controlling biophysical properties of these channels. This single amino acid substitution alters the biophysical properties of $hNa_v1.7$ in a manner, similar to that of other IEM mutations, that is consistent with rendering nociceptive DRG neurons hyperexcitable (Dib-Hajj et al 2005; Harty et al 2006; Rush et al 2006).

Ten erythromelalgia mutations in $Na_v1.7$ have been previously reported in families, and in sporadic cases where the mutation appears de novo (Yang et al., 2004; Dib-Hajj et al., 2005; Drenth et al., 2005; Michiels et al., 2005; Han et al., 2006; Harty et al., 2006; Lee et al., 2007; Takahashi et al., 2007), with half of these mutations identified in domain II. One mutation, L823R, increases the number of positively charged residues in the DII/S4 segment (Takahashi et al., 2007), three mutations (L858F, L858H, I848T) are located within DII/S4-S5 linker (Yang et al., 2004; Drenth et al., 2005; Han et al., 2006), and one mutation, A863P, in DII/S5 (Harty et al., 2006). The new mutation V872G is eight residues distal to A863P, near the C-terminus of DII/S5 (see Fig. 1). The disproportionate occurrence of mutations in the DII/S4-S5 linker and DII/S5 is consistent with an important functional role of these channel segments in channel activation, and suggests that other mutations in this region should cause channelopathies.

Whole-cell voltage-clamp studies show that the V872G substitution causes a ~10 mV hyperpolarizing shift in $V_{1/2,activation}$, slower deactivation kinetics, and larger ramp currents. The location of V872 near the C-terminal end of DII/S5 may influence the folding of the long S5–S6 extracellular linker that contributes residues to the selectivity filter of the channel (Catterall, 2000), possibly through an allosteric effect. However, the reversal potentials of wild-type and mutant channels were not significantly different, indicating that this mutation does not compromise the channels' selectivity for sodium ions. In addition to the hyperpolarizing shift in voltage-dependence of activation, the mutant channels activate with faster kinetics compared to wild-type channels, a change that out-paces the faster inactivation of the mutant channels (which, if not opposed by faster activation, would reduce excitability). By analogy to the conserved glycine residues within the S6 segments of sodium channels which have been shown to play a key structural role by permitting the splaying of S6 during channel activation (Zhao et al., 2004a; Zhao et al., 2004b), V872G may influence the bending of DII/S5 in the mutant channel. Glycine residue (G873), located immediately adjacent to V872G mutation, is conserved in all sodium channels (Fig. 1), and the presence of two glycine residues side-by-side may allow more bending of the S5 segment with a resultant effect on channel activation.

Transmembrane S5 segments contribute to the pore region of sodium channels, and are thus sensitive to amino acid substitutions (Cummins et al., 1993; Bendahhou et al., 1999; Wu et al., 2001; Harty et al., 2006; Keller et al., 2006). Moreover, several mutations in S5 segments of domains II, III and IV of $Na_v1.1$ render the channel non-functional (Lossin et al., 2003; Fukuma et al., 2004; Rhodes et al., 2004), further supporting an important role of this segment in channel function. However, biophysical properties of channels carrying mutations in S5 segments appear to depend on which domain carries the mutation and the relative position of the mutation within the S5 segment. For example, the $Na_v1.4$ mutants T704M in DII/S5 and I1495F in DIV/S5 shift voltage-dependence of activation in a hyperpolarizing direction (Cummins et al., 1993; Bendahhou et al., 1999), while L266V in DI/S5 produces a depolarizing shift in steady-state inactivation but no effect on activation (Wu et al., 2001); mutant F1344S in DIII/S5 in $Na_v1.5$ causes Brugada syndrome and shifts activation in a depolarizing direction (Keller et al., 2006); mutant A863P in $Na_v1.7$ causes erythromelalgia and shifts voltage-dependence of activation in a hyperpolarizing direction and produces a depolarizing shift in steady-state inactivation (Harty et al., 2006). These studies show that mutations in S5 of sodium channels may have diverse effects, and must be verified experimentally.

The V872G mutation does not alter the voltage-dependence of steady-state inactivation. In contrast A863P, the other erythromelalgia mutation in DII/S5 (Fig. 1), causes an 8 mV hyperpolarizing shift in the $V_{1/2}$ of activation and a 10 mV depolarizing shift in the $V_{1/2}$ of steady-state inactivation (Harty et al., 2006). The differential effect of the two mutations within the same S5 may reflect the position of each mutation relative to the extra- or intra-cellular vestibule of the channel, with the cytoplasmic-proximal A863P

mutation affecting the interaction of the inactivation peptide with its receptor, perhaps via an allosteric effect by the proline-mediated bending of the helix.

The changes in the biophysical properties of V872G mutant $Na_V1.7$ channels are expected to contribute to hyperexcitability of DRG neurons which underlies painful symptoms of erythromelalgia. Computer simulation studies have suggested that the hyperpolarized shift in activation is sufficient to induce repetitive firing in DRG neurons (Sheets et al., 2007). Recently, we have shown that the erythromelalgia mutant channel L858H, which alters channel activation but not steady-state-inactivation (Cummins et al., 2004), lowers the threshold for single action potentials and increases frequency of action potential firing in DRG neurons (Rush et al., 2006). Thus changes in the biophysical properties of the V872G mutant channels can explain the molecular pathophysiology of neuropathic pain in this patient.

The patient described in this report displayed a favorable clinical response to treatment with mexiletine. The V872G mutation in this patient did not alter the tonic inhibition of the channel by mexiletine. However, high frequency (5 Hz) stimulation to −10 mV revealed a stronger use-dependent fall-off of current for V872G channels following exposure to mexiletine, compare to wild-type channels. Because of the hyperpolarizing shift in activation of V872G, a greater proportion of the mutant channels will be opened and then inactivated at potentials of the membrane during the initial parts of an action potential, prior to reaching +20 mV where activation for both V872G and wild-type channels are maximal, allowing a differential effect of mexiletine on the mutant channels, as we observed. This could underlie the therapeutic response to mexiletine that was observed clinically, in the context of similar dose–response curves for the mutant and wild-type channels at low stimulation frequencies. A similar mode of action might underlie the therapeutic response to lidocaine and mexiletine that has been observed (Nathan et al 2005) with occasional other IEM mutations such as A863P which also shift activation in a hyperpolarizing direction (Harty et al 2006). The increased use-dependent effect of mexilitine on V872G, compared to wild-type channels, suggests that use-dependent effects may be more important than tonic block of mutant $Na_v1.7$ channels in the treatment of IEM. Since some inactivated IEM mutant channels display altered sensitivities to sodium channel blockers (Sheets et al., 2007), the different responses of patients with different mutations to treatment with these drugs (Harty et al 2006) is not surprising. The observation of a degree of sensitivity of some patients carrying IEM mutations to treatment with local anesthetics suggests that, for at least some patients with IEM, genomically-targeted therapy may at some time be feasible. Moreover, the long-lasting improvement in this patient after a one month period of treatment with mexiletine leads us to suggest the possibility that, via a mechanism that is not yet understood, transient attenuation of DRG neuron hyperexcitability at early stages of IEM may have long-lasting effects.

Acknowledgments

We thank Emmanuella Eastman and Bart Toftness for excellent technical assistance and Dr. Mark Estacion for helpful discussion. This work was supported by the Medical Research Service and Rehabilitation Research Service, Dept. of Veterans Affairs and by grants from the National Multiple Sclerosis Society and the Erythromelalgia Association (SDH and SGW); National Program for New Century Excellent Talents in University (NCET-06-0015) and National Natural Science Foundation (Grant 30400168) (YY). The Center for Neuroscience and Regeneration Research is a Collaboration of the Paralyzed Veterans of America and the United Spinal Association with Yale University. We thank the family members for participating in this study.

References

Ahmad, S., Dahllund, L., Eriksson, A.B., Hellgren, D., Karlsson, U., Lund, P.E., Meijer, I.A., Meury, L., Mills, T., Moody, A., Morinville, A., Morten, J., O'Donnell, D., Raynoschek, C., Salter, H., Rouleau, G.A., Krupp, J.J., 2007. A stop codon mutation in SCN9A causes lack of pain sensation. Hum. Mol. Genet. 16, 2114–2121.

Bendahhou, S., Cummins, T.R., Tawil, R., Waxman, S.G., Ptacek, L.J., 1999. Activation and inactivation of the voltage-gated sodium channel: role of segment S5 revealed by a novel hyperkalaemic periodic paralysis mutation. J. Neurosci. 19, 4762–4771.

Catterall, W.A., 2000. From ionic currents to molecular mechanisms: the structure and function of voltage-gated sodium channels. Neuron 26, 13–25.

Cheng, X., Dib-Hajj, S.D., Tyrrell, L., Waxman, S.G., 2008. Mutation I136V alters electrophysiological properties of the NaV1.7 channel in a family with onset of erythromelalgia in the second decade. Mol. Pain 4, 1.

Choi, J.S., Dib-Hajj, S.D., Waxman, S.G., 2006. Inherited erythermalgia. Limb pain from an S4 charge-neutral Na channelopathy. Neurology 67, 1563–1567.

Cox, J.J., Reimann, F., Nicholas, A.K., Thornton, G., Roberts, E., Springell, K., Karbani, G., Jafri, H., Mannan, J., Raashid, Y., Al-Gazali, L., Hamamy, H., Valente, E.M., Gorman, S., Williams, R., McHale, D.P., Wood, J.N., Gribble, F.M., Woods, C.G., 2006. An SCN9A channelopathy causes congenital inability to experience pain. Nature 444, 894–898.

Cummins, T.R., Dib-Hajj, S.D., Waxman, S.G., 2004. Electrophysiological properties of mutant Nav1.7 sodium channels in a painful inherited neuropathy. J. Neurosci. 24, 8232–8236.

Cummins, T.R., Zhou, J., Sigworth, F.J., Ukomadu, C., Stephan, M., Ptacek, L.J., Agnew, W.S., 1993. Functional consequences of a Na+ channel mutation causing hyperkalemic periodic paralysis. Neuron 10, 667–678.

Dib-Hajj, S.D., Cummins, T.R., Black, J.A., Waxman, S.G., 2007. From genes to pain: $Na_v1.7$ and human pain disorders. Trends Neurosci. 30, 555–563.

Dib-Hajj, S.D., Estacion, M., Jarecki, B.W., Tyrrell, L., Fisher, T.Z., Lawden, M., Cummins, T.R., Waxman, S.G., 2008. Paroxysmal extreme pain disorder M1627K mutations in human Nav1.7 renders DRG neurons hyperexcitable. Mol. Pain 4, 37.

Dib-Hajj, S.D., Rush, A.M., Cummins, T.R., Hisama, F.M., Novella, S., Tyrrell, L., Marshall, L., Waxman, S.G., 2005. Gain-of-function mutation in Nav1.7 in familial erythromelalgia induces bursting of sensory neurons. Brain 128, 1847–1854.

Drenth, J.P., Waxman, S.G., 2007. Mutations in sodium-channel gene SCN9A cause a spectrum of human genetic pain disorders. J. Clin. Invest. 117, 3603–3609.

Drenth, J.P., Te Morsche, R.H., Guillet, G., Taieb, A., Kirby, R.L., Jansen, J.B., 2005. SCN9A mutations define primary erythermalgia as a neuropathic disorder of voltage gated sodium channels. J. Invest. Dermatol. 124, 1333–1338.

Estacion, M., Dib-Hajj, S.D., Benke, P.J., te Morsche, R.H.M., Eastman, E.M., Macala, L.J., Drenth, J.P.H., Waxman, S.G., 2008. $Na_V1.7$ gain-of-function mutations as a continuum: A1632E displays physiological changes associated with erythromelalgia and paroxysmal extreme pain disorder mutations and produces symptoms of both disorders. J. Neurosci. 28, 11079–11088.

Fertleman, C.R., Baker, M.D., Parker, K.A., Moffatt, S., Elmslie, F.V., Abrahamsen, B., Ostman, J., Klugbauer, N., Wood, J.N., Gardiner, R.M., Rees, M., 2006. SCN9A mutations in paroxysmal extreme pain disorder: allelic variants underlie distinct channel defects and phenotypes. Neuron 52, 767–774.

Fukuma, G., Oguni, H., Shirasaka, Y., Watanabe, K., Miyajima, T., Yasumoto, S., Ohfu, M., Inoue, T., Watanachai, A., Kira, R., Matsuo, M., Muranaka, H., Sofue, F., Zhang, B., Kaneko, S., Mitsudome, A., Hirose, S., 2004. Mutations of neuronal voltage-gated Na+ channel alpha 1 subunit gene SCN1A in core severe myoclonic epilepsy in infancy (SMEI) and in borderline SMEI (SMEB). Epilepsia 45, 140–148.

Goldberg, Y., Macfarlane, J., Macdonald, M., Thompson, J., Dube, M.P., Mattice, M., Fraser, R., Young, C., Hossain, S., Pape, T., Payne, B., Radomski, C., Donaldson, G., Ives, E., Cox, J., Younghusband, H., Green, R., Duff, A., Boltshauser, E., Grinspan, G., Dimon, J., Sibley, B., Andria, G., Toscano, E., Kerdraon, J., Bowsher, D., Pimstone, S., Samuels, M., Sherrington, R., Hayden, M., 2007. Loss-of-function mutations in the $Na_v1.7$ gene underlie congenital indifference to pain in multiple human populations. Clin. Genet. 71, 311–319.

Han, C., Rush, A.M., Dib-Hajj, S.D., Li, S., Xu, Z., Wang, Y., Tyrrell, L., Wang, X., Yang, Y., Waxman, S.G., 2006. Sporadic onset of erythermalgia: a gain-of-function mutation in Nav1.7. Ann. Neurol. 59, 553–558.

Harty, T.P., Dib-Hajj, S.D., Tyrrell, L., Blackman, R., Hisama, F.M., Rose, J.B., Waxman, S.G., 2006. $Na_V1.7$ mutant A863P in erythromelalgia: effects of altered activation and steady-state inactivation on excitability of nociceptive dorsal root ganglion neurons. J. Neurosci. 26, 12566–12575.

Keller, D.I., Huang, H., Zhao, J., Frank, R., Suarez, V., Delacretaz, E., Brink, M., Osswald, S., Schwick, N., Chahine, M., 2006. A novel SCN5A mutation, F1344S, identified in a patient with Brugada syndrome and fever-induced ventricular fibrillation. Cardiovasc. Res. 70, 521–529.

Klugbauer, N., Lacinova, L., Flockerzi, V., Hofmann, F., 1995. Structure and functional expression of a new member of the tetrodotoxin-sensitive voltage-activated sodium channel family from human neuroendocrine cells. EMBO J. 14, 1084–1090.

Lampert, A., Dib-Hajj, S.D., Tyrrell, L., Waxman, S.G., 2006. Size matters: Erythromelalgia mutation S241T in Nav1.7 alters channel gating. J. Biol. Chem. 281, 36029–36035.

Lee, M.J., Yu, H.S., Hsieh, S.T., Stephenson, D.A., Lu, C.J., Yang, C.C., 2007. Characterization of a familial case with primary erythromelalgia from Taiwan. J. Neurol. 254, 210–214.

Lossin, C., Wang, D.W., Rhodes, T.H., Vanoye, C.G., George Jr, A.L., 2002. Molecular basis of an inherited epilepsy. Neuron 34, 877–884.

Lossin, C., Rhodes, T.H., Desai, R.R., Vanoye, C.G., Wang, D., Carniciu, S., Devinsky, O., George Jr, A.L., 2003. Epilepsy-associated dysfunction in the voltage-gated neuronal sodium channel SCN1A. J. Neurosci. 23, 11289–11295.

Michiels, J.J., te Morsche, R.H., Jansen, J.B., Drenth, J.P., 2005. Autosomal dominant erythermalgia associated with a novel mutation in the voltage-gated sodium channel alpha subunit Nav1.7. Arch. Neurol. 62, 1587–1590.

Nathan, A., Rose, J.B., Guite, J.W., Hehir, D., Milovcich, K., 2005. Primary erythromelalgia in a child responding to intravenous lidocaine and oral mexiletine treatment. Pediatrics 115, e504–e507.

Rhodes, T.H., Lossin, C., Vanoye, C.G., Wang, D.W., George Jr, A.L., 2004. Noninactivating voltage-gated sodium channels in severe myoclonic epilepsy of infancy. Proc. Natl. Acad. Sci. U. S. A. 101, 11147–11152.

Rush, A.M., Dib-Hajj, S.D., Liu, S., Cummins, T.R., Black, J.A., Waxman, S.G., 2006. A single sodium channel mutation produces hyper- or hypoexcitability in different types of neurons. Proc. Natl. Acad. Sci. U. S. A. 103, 8245–8250.

Sheets, P.L., Jackson Ii, J.O., Waxman, S.G., Dib-Hajj, S., Cummins, T.R., 2007. A Nav1.7 channel mutation associated with hereditary erythromelalgia contributes to neuronal hyperexcitability and displays reduced lidocaine sensitivity. J. Physiol. (Lond) 581, 1019–1031.

Takahashi, K., Saitoh, M., Hoshino, H., Mimaki, M., Yokoyama, Y., Takamizawa, M., Mizuguchi, M., Lin, Z.M., Yang, Y., Igarashi, T., 2007. A case of primary erythermalgia, wintry hypothermia and encephalopathy. Neuropediatrics 38, 157–159.

Waxman, S.G., 2007. Channel, neuronal and clinical function in sodium channelopathies: from genotype to phenotype. Nat. Neurosci. 10, 405–409.

Wu, F.F., Takahashi, M.P., Pegoraro, E., Angelini, C., Colleselli, P., Cannon, S.C., Hoffman, E.P., 2001. A new mutation in a family with cold-aggravated myotonia disrupts Na(+) channel inactivation. Neurology 56, 878–884.

Yang, Y., Wang, Y., Li, S., Xu, Z., Li, H., Ma, L., Fan, J., Bu, D., Liu, B., Fan, Z., Wu, G., Jin, J., Ding, B., Zhu, X., Shen, Y., 2004. Mutations in SCN9A, encoding a sodium channel alpha subunit, in patients with primary erythermalgia. J. Med. Genet. 41, 171–174.

Zhao, Y., Scheuer, T., Catterall, W.A., 2004a. Reversed voltage-dependent gating of a bacterial sodium channel with proline substitutions in the S6 transmembrane segment. Proc. Natl. Acad. Sci. U. S. A. 101, 17873–17878.

Zhao, Y., Yarov-Yarovoy, V., Scheuer, T., Catterall, W.A., 2004b. A gating hinge in na(+) channels; a molecular switch for electrical signaling. Neuron 41, 859–865.